The Plant Cell, Vol. 20: 2860–2875, October 2008, www.plantcell.org © 2008 American Society of Plant Biologists

NIP6;1 Is a Boric Acid Channel for Preferential Transport of Boron to Growing Shoot Tissues in *Arabidopsis* [W]

Mayuki Tanaka,[a,b] Ian S. Wallace,[c] Junpei Takano,[b] Daniel M. Roberts,[c] Toru Fujiwara[b,d,1]

[a] Graduate School of Agricultural and Life Science, University of Tokyo, Yayoi, Bunkyo-ku, Tokyo 113-8657, Japan
[b] Biotechnology Research Center, University of Tokyo, Yayoi, Bunkyo-ku, Tokyo 113-8657, Japan
[c] Department of Biochemistry, Cellular, and Molecular Biology and Center of Excellence in Structural Biology, University of Tennessee, Knoxville, Tennessee 37996
[d] Solution Oriented Research for Science and Technology, Japan Science and Technology Agency, 3-4-15 Nihonbashi, Tokyo 103-0027, Japan

Boron (B) in soil is taken up by roots through NIP5;1, a boric acid channel, and is loaded into the xylem by BOR1, a borate exporter. Here, the function of *Arabidopsis thaliana NIP6;1*, the most similar gene to *NIP5;1*, was studied. NIP6;1 facilitates the rapid permeation of boric acid across the membrane but is completely impermeable to water. *NIP6;1* transcript accumulation is elevated in response to B deprivation in shoots but not in roots. *NIP6;1* promoter–β-glucuronidase is predominantly expressed in nodal regions of shoots, especially the phloem region of vascular tissues. Three independently identified T-DNA insertion lines for the *NIP6;1* gene exhibited reduced expansion of young rosette leaves only under low-B conditions. B concentrations are reduced in young rosette leaves but not in the old leaves of these mutants. Taken together, these data strongly suggest that NIP6;1 is a boric acid channel required for proper distribution of boric acid, particularly among young developing shoot tissues. We propose that NIP6;1 is involved in xylem–phloem transfer of boric acid at the nodal regions and that the water-tight property of NIP6;1 is important for this function. It is proposed that during evolution, NIP5;1 and NIP6;1 were diversified in terms of both the specificity of their expression in plant tissues and their water permeation properties, while maintaining their ability to be induced under low B and their boric acid transport activities.

INTRODUCTION

Boric acid is a small molecule with the central boron (B) atom possessing three valence electrons. The molecular radius of boric acid is 2.573 Å, similar to those of some other small uncharged molecules such as urea (2.618 Å). Boric acid is a very weak Lewis acid with pK_a of 9.24. B in neutral solution is mostly present as boric acid (H_3BO_3) (reviewed in Marschner, 1995; Woods, 1996).

B is an essential element not only for vascular plants but also for diatoms, cyanobacteria, and a number of species of marine algal flagellates (Warington, 1923; Loomis and Durst, 1992; Marschner, 1995). B is also required by animals, including zebrafish (*Danio rerio*), trout (*Oncorhynchus mykiss*) (Rowe and Eckhert, 1999), and frogs (*Xenopus laevis*) (Fort et al., 1998).

One of the primary functions of B in plants is to serve in the cross-linking of rhamnogalacturonan-II (RG-II), a component of cell wall pectic polysaccharides. RG-II is an essential component of a stable three-dimensional pectic network, and borate forms a cross-link with apiose residues of RG-II (reviewed in O'Neill et al., 2001, 2004).

[1] Address correspondence to atorufu@mail.ecc.u-tokyo.ac.jp.
The author responsible for distribution of materials integral to the findings presented in this article in accordance with the policy described in the Instructions for Authors (www.plantcell.org) is: Toru Fujiwara (atorufu@mail.ecc.u-tokyo.ac.jp).
[W] Online version contains Web-only data.
www.plantcell.org/cgi/doi/10.1105/tpc.108.058628

Symptoms of B deficiency occur mainly in growing or expanding organs in the plant body. Under B-deficient conditions, leaf expansion and root elongation, apical dominance, flower development, and fruit and seed set are inhibited (Marschner, 1995; Dell and Huang, 1997; Shorrocks, 1997). These B deficiency symptoms suggest that B is relatively immobile in the phloem in many plant species.

Recent reports suggest that B can be retranslocated from old tissues to young tissues or can be preferentially transported to sink tissues under B deficiency. Some plant species produce and translocate significant amounts of sugar alcohols, including mannitol and sorbitol. Because sugar alcohols contain *cis*-hydroxyl groups, they can readily bind to boric acid (forming a poly-B complex) and allow B to be retranslocated through phloem (Brown and Hu, 1996; Brown and Shelp, 1997). Although retranslocation of B is limited in sugar alcohol–nonproducing plants, Huang et al. (2008) recently demonstrated that B is retranslocated from old tissues to young tissues in response to short-term B deficiency in white lupin (*Lupinus albus*), which does not produce sugar alcohols.

On the other hand, some sugar alcohol–nonproducing plants, including *Arabidopsis thaliana* (Noguchi et al., 2000; Takano et al., 2001), broccoli (*Brassica oleracea*) and lupin (Shelp et al., 1998), canola (*Brassica napus*) (Stangoulis et al., 2001a), and sunflower (*Helianthus annuus*) (Matoh and Ochiai, 2005) preferentially transport newly acquired B to sink tissues under low-B conditions. Mechanisms of the preferential transport of B remain elusive.

It has long been believed that B is passively transported; that is, the B transport rate is in proportion to the transmembrane concentration gradients. This was based on the relatively high permeability of boric acid to lipid bilayers, as boric acid is a noncharged molecule (Raven, 1980). Permeability coefficients of boric acid were experimentally determined in the membrane vesicles isolated from squash roots (*Cucurbita pepo*) (Dordas, et al., 2000) and giant internodal cells of the charophyte alga (*Chara corallina*) (Stangoulis et al., 2001b). It was suggested that simple diffusive transport of boric acid across the lipid bilayer is the major portion of transmembrane B transport and can satisfy the needs of the plant demand for B under conditions of a relatively high B supply.

However, recent studies revealed the importance of transport proteins in transmembrane B transport (reviewed in Tanaka and Fujiwara, 2008; Takano et al., 2008), *Arabidopsis* BOR1 was identified as a B efflux transporter capable of transporting B against the B concentration gradient and is required for normal growth under low-B conditions (Takano et al., 2002). Furthermore, NIP5;1, an aquaporin-like protein, was shown to be a boric acid channel for facilitated B transport across the membrane (Takano et al., 2006). These studies demonstrated the significance of transport proteins for B transport under conditions of B limitation.

NIP5;1 belongs to the Major Intrinsic Protein (MIP) family. MIPs are present in mammals, amphibians, yeast, bacteria, and plants and are known to facilitate the passive flow of small uncharged molecules such as glycerol, urea, and formamide as well as water. Thirty-five MIP genes are present in the *Arabidopsis* genome. Plant MIPs can be subdivided into four distinct groups: the tonoplast intrinsic proteins, the plasma membrane intrinsic proteins (PIPs), the small basic intrinsic proteins, and the nodulin

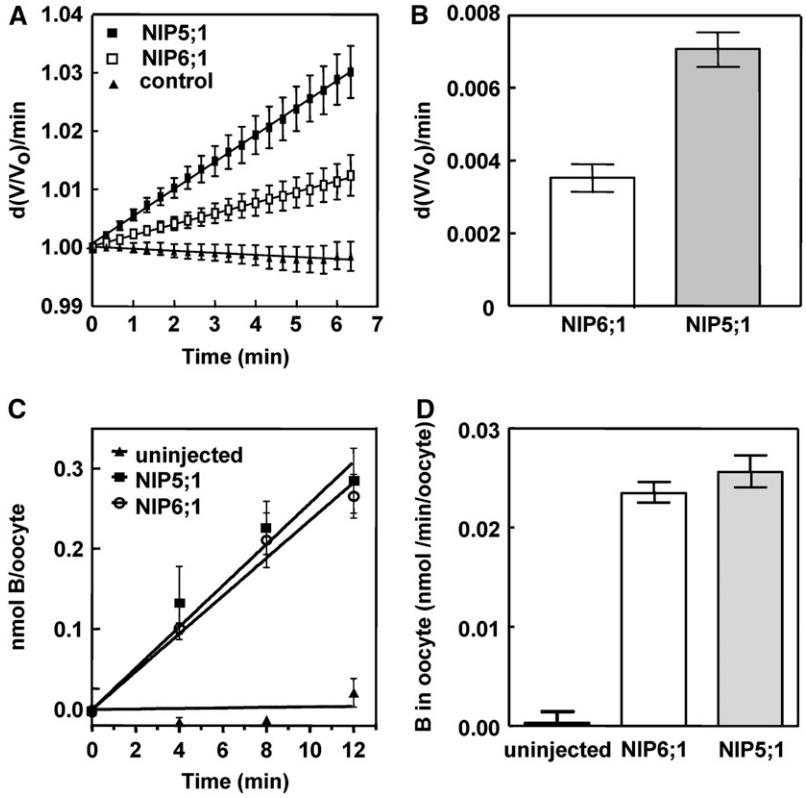

Figure 1. NIP6;1 Facilitates Boric Acid Transport in *Xenopus* Oocytes.

Xenopus oocytes were injected with *NIP6;1* or *NIP5;1* cRNA (46 ng) and assayed for B transport at 3 d after injection.

(A) Osmotic boric acid swelling assay. *NIP5;1* and *NIP6;1* cRNA–injected or uninjected control oocytes were incubated in modified Ringer's solution (190 mosmol/kg) with 200 mM boric acid. The initial swelling rates were measured by video microscopy. Data shown are means ± SE (n = 17 to 24 oocytes).

(B) Summary of swelling rates for *NIP5;1*- and *NIP6;1*-injected oocytes after background correction of the basal rate of nonspecific boric acid diffusion through the oocyte plasma membrane (from uninjected oocytes). The difference between the NIP5;1 and NIP6;1 rates is significant ($P < 0.05$ by an unpaired Student's t test).

(C) Time course showing direct boric acid uptake by oocytes assayed by ICP-MS. Oocytes injected with *NIP5;1* or *NIP6;1* cRNAs and uninjected control oocytes were incubated in Ringer's solution supplemented with 2 mM boric acid. Mean values ± SE are shown (n = 4).

(D) Comparison of linear rates of boric acid uptake with error bars showing SE. The rates of uptake by the NIP5;1 and NIP6;1 oocytes were significantly different from those of control oocytes ($P < 0.001$ by Student's t test).

26 (NOD26)–like intrinsic proteins (NIPs) (reviewed in Johanson et al., 2001; Tyerman et al., 2002; Zardoya, 2005; Maurel, 2007).

The NIP subfamily is specific for plants. Nine *NIP* genes are present in *Arabidopsis*. Some NIPs have been shown to be multifunctional channels that mediate the transport of small uncharged molecules such as glycerol and urea as well as water (reviewed in Wallace et al., 2006). The NIP family is further subdivided into two aromatic/Arg (ar/R) region subgroups (I and II), based on the conservation of two disparate sequence motifs in the selectivity filter in these two subgroups of proteins (Wallace and Roberts, 2004). NIP5;1 belongs to subgroup II. The ar/R region of NIP subgroup I is similar to NOD26, an aquaglyceroporin, whereas NIP subgroup II is more divergent.

NIP5;1 is a plasma membrane boric acid transporter expressed in root epidermal, cortical, and endodermal cells. Expression of the *NIP5;1* transcript is transcriptionally upregulated in response to B deprivation. NIP5;1 is involved in B uptake from the root surface under conditions of B limitation as a major boric acid channel (Takano et al., 2006).

It is possible that other members of the NIP family are also involved in B transport. *NIP6;1*, is the most similar gene to *NIP5;1* in *Arabidopsis*. NIP5;1 and NIP6;1 belong to NIP subgroup II, and computational homology modeling shows that NIP6;1 is predicted to possess a wider pore at the ar/R region compared with NIP subgroup I, and the three-dimensional structure is predicted to be similar to that of NIP5;1 (Wallace and Roberts, 2004). This suggests that NIP6;1 may be a boric acid channel, as was the case of NIP5;1. In addition, microarray data indicate that *NIP6;1* is mainly expressed in stems (Zimmermann et al., 2004), suggesting the possible involvement of NIP6;1 in B transport in shoots. In this study, we demonstrate that NIP6;1 possesses a boric acid channel activity and that NIP6;1 functions in B transport in developing shoot tissues of *Arabidopsis*.

RESULTS

B Transport Activity in *Xenopus* Oocytes

Phylogenetic analysis of the predicted amino acid sequences revealed that among the nine *Arabidopsis NIP* genes, NIP6;1 is the most similar to NIP5;1 (66.4% amino acid sequence identity and 83.1% similarity) (Wallace and Roberts, 2004).

In a previous report, we showed that NIP5;1 transports boric acid efficiently in *Xenopus* oocytes (Takano et al., 2006). We also demonstrated that NIP6;1 had a transport selectivity for uncharged molecules such as glycerol, formamide, and urea but was impermeable to water (Wallace and Roberts, 2005). Due to the similarities between NIP5;1 and NIP6;1, we decided to use the *Xenopus* expression system to investigate whether NIP6;1 is also a boric acid transporter. In these experiments, NIP5;1 was used as a control for B transport (Takano et al., 2006).

In an osmotic boric acid swelling assay, *NIP6;1* and *NIP5;1* copy RNA (cRNA)–injected and control oocytes were placed in modified, isoosmotic Ringer's solution (190 mosmol/kg) in which NaCl was replaced with boric acid. Under these assay conditions, boric acid transport into oocytes results in an osmotic gradient that subsequently drives water movement into oocytes, causing an increase in cell volume and oocyte swelling. The initial rate of oocyte swelling is a function of two parameters: the solute permeability for boric acid and the osmotic water permeability (P_f) of the oocyte plasma membrane.

NIP6;1- and NIP5;1-expressing oocytes showed significant swelling upon exposure to boric acid, while negative control oocytes (uninjected or mock-injected oocytes) showed little or no swelling under the same conditions (Figures 1A and 1B; see Supplemental Figure 1A online). In addition, pretreatment of NIP5;1- and NIP6;1-injected oocytes with the aquaporin channel blocker $HgCl_2$ reduced boric acid–induced swelling to levels observed in uninjected oocytes (see Supplemental Figure 1B online). Overall, these properties are consistent with the facilitated transport of boric acid and suggest that NIP6;1 is a boric acid channel, similar to NIP5;1.

The rate of oocyte swelling was slower in NIP6;1-expressing oocytes than in NIP5;1-expressing oocytes (Figure 1A), even though protein gel blot analysis shows a similar expression level of both proteins in oocyte lysates (see Supplemental Figure 2 online). Boric acid uptake was further verified by directly quantifying the amount of boric acid taken up by oocytes using inductively coupled plasma–mass spectrometry (ICP-MS). Figure 1C shows a time course of boric acid uptake for NIP5;1 and NIP6;1 oocytes compared with uninjected controls. Both NIP5;1- and NIP6;1-injected oocytes show linear boric acid uptake rates that are over 50-fold higher than those of uninjected control oocytes (Figures 1C and 1D).

To compare the water transport properties of NIP6;1 and NIP5;1, a P_f assay was conducted. The water transport rate of NIP6;1-expressing oocytes was indistinguishable from that of control oocytes, with both showing a low P_f characteristic of diffusion across the bare bilayer. By contrast, oocytes expressing NIP5;1 showed facilitated water transport that was twofold

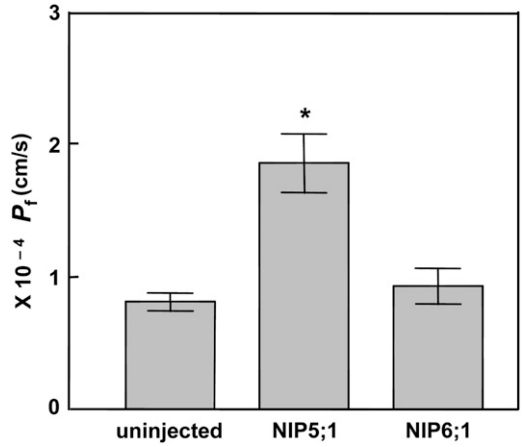

Figure 2. Comparison of the P_f of NIP6;1 and NIP5;1 in *Xenopus* Oocytes.

The P_f in the oocyte-swelling assay was determined for oocytes expressing NIP6;1 and NIP5;1 or uninjected oocytes. Error bars show SE (n = 11 oocytes). The asterisk denotes a significant difference from uninjected oocytes ($P < 0.05$ by Student's t test).

higher than that of control and NIP6;1-expressing oocytes (Figure 2). These observations account for the apparent differences in boric acid–induced swelling rate between NIP5;1 and NIP6;1 oocytes. Overall, the transport analyses indicate that both NIP5;1 and NIP6;1 are boric acid transporters but are different in terms of water transport activities, with NIP6;1 forming a water-tight boric acid transport channel.

Subcellular Localization of NIP6;1

Soybean (*Glycine max*) NOD26, the archetype of the NIP family, is localized on the symbiosome membrane of nitrogen-fixing root nodules (Fortin et al., 1987; Weaver et al., 1991), but the subcellular localization data for nonsymbiotic NIPs are limited. *Arabidopsis* NIP5;1 (Takano et al., 2006) is localized on the plasma membrane, and NIP2;1 is reported to be localized on the plasma membrane (Choi and Roberts, 2007) and the endoplasmic reticulum (Mizutani et al., 2006). To investigate the subcellular localization of NIP6;1, an expression construct (referred to as *35S-GFP-NIP6;1*) of *NIP6;1* fused to the C terminus of the green fluorescent protein (*GFP*) under the control of a cauliflower mosaic virus 35S RNA promoter (*P35S*) was introduced into *Arabidopsis* plants. Transgenic plants carrying the promoter of *NIP5;1* fused to *GFP* (referred to as *Pro-NIP5;1-GFP*) were used

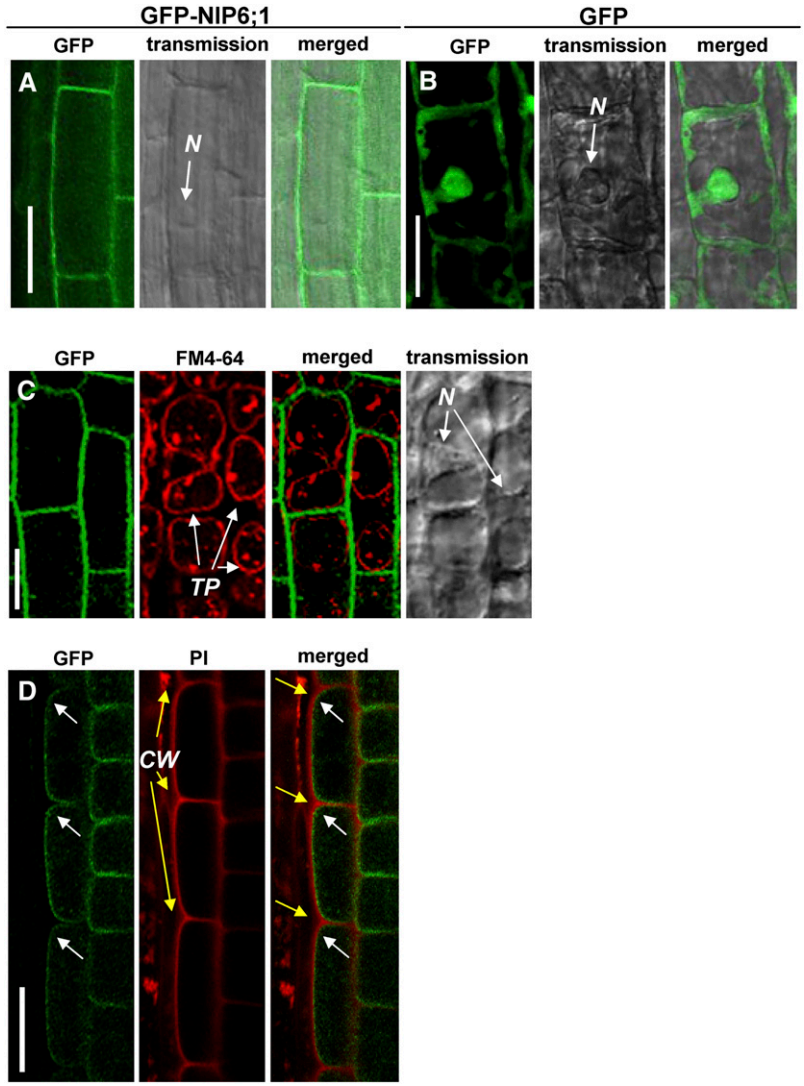

Figure 3. NIP6;1 Is Localized on the Plasma Membrane in Transgenic *Arabidopsis* Seedlings.

35S-GFP-NIP6;1 (**[A]**, **[C]**, and **[D]**) and *Pro-NIP5;1-GFP* **(B)** constructs were introduced into *Arabidopsis*, and cells were visualized using confocal microscopy and Nomarski optics. The images shown are from the root elongation zone (**[A]**, **[B]**, and **[D]**) or root tips **(C)** of 10-d-old transgenic plants. In **(C)**, tonoplasts were stained red with FM-64. In **(D)**, cell walls were counterstained red with propidium iodide (PI) and then treated with 0.5 M mannitol solution to induce plasmolysis. White and yellow arrows in **(D)** indicate the cell periphery and cell wall, respectively. *CW*, cell walls; *N*, nucleus; *TP*, tonoplast. Bars = 50 μm in **(A)** to **(C)** and 20 μm in **(D)**.

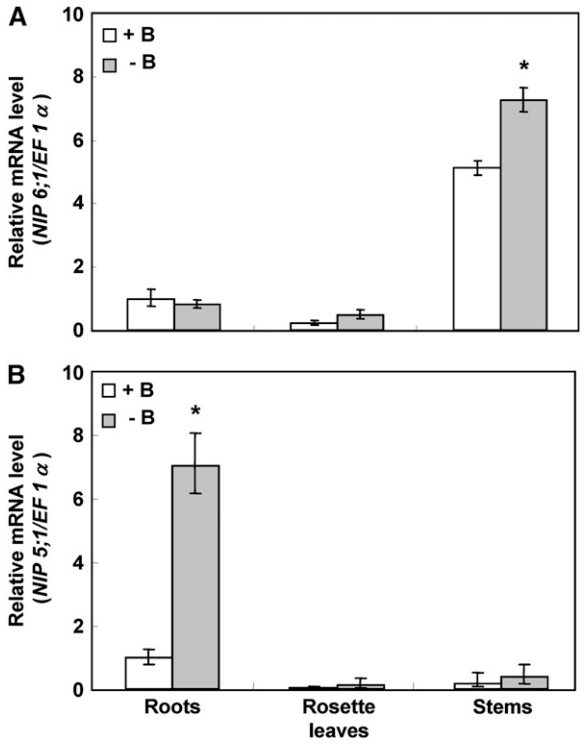

Figure 4. Accumulation of mRNA of *NIP6;1* Is Upregulated by B Limitation in Rosette Leaves.

B-dependent *NIP6;1* **(A)** and *NIP5;1* **(B)** mRNA accumulation in roots, rosette leaves, and stems was quantified by Q-PCR analysis. Plants (Col-0) grown for 46 d at 100 μM B were transferred to medium containing 0.1 μM (−B) or 100 μM (+B) B for 24 h. Means of three biological replicates ± SE (n = 3) are shown. Asterisks show significant differences from the +B condition ($P < 0.05$ by Student's t test).

as a control for subcellular localization of free GFP. NIP6;1-dependent green fluorescence in the root elongation zone and root tips of three independent transgenic lines was observed. Representative images are shown in Figure 3. GFP fluorescence in cells expressing GFP-NIP6;1 was localized on the cell periphery; by contrast, GFP fluorescence of cells expressing free GFP was detected at the nucleus and cell periphery in the root elongation zone (Figures 3A and 3B).

To exclude the possibility that GFP fluorescence is associated with the tonoplast, transgenic plants were stained with FM4-64 for 5 min and observed after 18 h of incubation in the dark. Under this condition, FM4-64 signals were associated with the tonoplast, while GFP fluorescence remained at the cell periphery of the root tips (Figure 3C), confirming that the GFP florescence is not associated with the tonoplast. To further confirm the plasma membrane localization of NIP6;1, transgenic plants were stained with propidium iodide for cell wall staining and then treated with 0.5 M mannitol solution to induce plasmolysis. GFP fluorescence was separated from the propidium iodide signal at the root elongation zone (Figure 3D), confirming that NIP6;1 is localized to the plasma membrane.

NIP6;1 Transcript Accumulation

Microarray data indicate that *NIP5;1* is mainly expressed in roots, whereas *NIP6;1* is mainly expressed in stems (Zimmermann et al., 2004). Accumulation of mRNA of *NIP5;1* was increased in response to B limitation in roots, and the mRNA accumulation of *NIP5;1* was enhanced 10-fold under B-limiting conditions (Takano et al., 2006). Therefore, we wanted to determine whether the *NIP6;1* transcript was subject to a similar response to B limitation.

To test for B-dependent regulation of *NIP6;1*, quantitative RT-PCR (Q-PCR) was conducted. Wild-type plants (ecotype Col-0) were grown in solid medium containing 100 μM B (+B) for 27 d and then transferred to hydroponic culture solutions containing 100 μM B for 19 d. The plants were then incubated for an additional 24-h period in medium containing either 100 or 0.1 μM B (−B) prior to Q-PCR analysis.

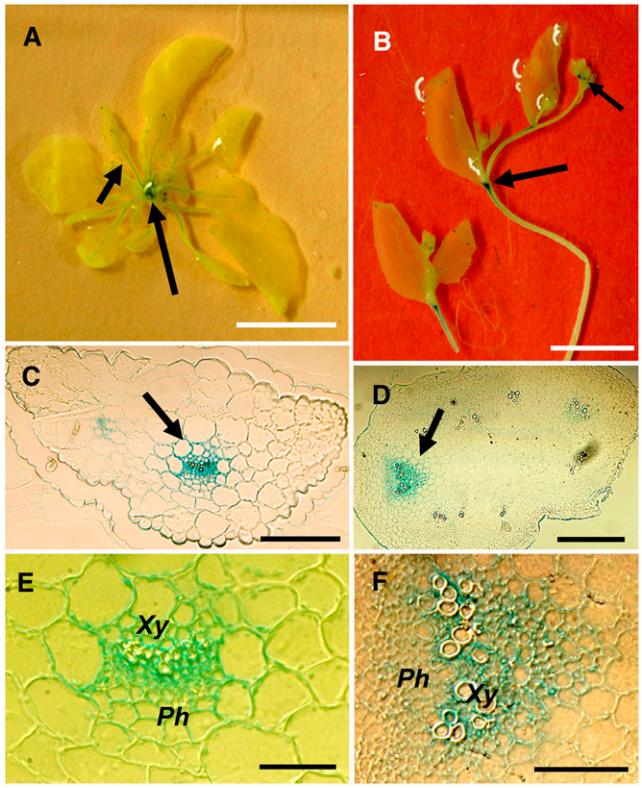

Figure 5. Analysis of GUS Staining in *Pro-NIP6;1-GUS* Transgenic Plants.

Pro-NIP6;1-GUS transgenic plants were grown hydroponically for 4 weeks in medium supplied with 30 μM B under long-day conditions and were stained with 5-bromo-4-chloro-3-indolyl-β-D-glucuronic acid. Whole plant **(A)**, stems **(B)**, cross section of the petiole of a young leaf **(C)**, the node **(D)**, close-up of the petiole in the vascular strand region **(E)**, and close-up of the node in the vascular strand region **(F)** are shown. *Ph*, phloem; *Xy*, xylem. Each photographic series (**[A]-[C]-[E]**, **[B]-[D]-[F]**) illustrates the same location at different focal planes: petiole (**[A]-[C]-[E]**) and node (**[B]-[D]-[F]**). Arrows indicate GUS staining. Bars = 10 mm in **(A)** and **(B)**, 100 μm in **(C)** and **(D)**, and 50 μm in **(E)** and **(F)**.

NIP6;1 transcript levels in stems were higher than those in roots and rosette leaves, in contrast with those of the *NIP5;1* transcript, which accumulated predominantly in roots (Figure 4). *NIP6;1* mRNA accumulation in stems was increased by 1.4-fold under conditions of B limitation (−B) compared with that under high-B conditions (+B), while the response was not evident in roots and rosette leaves (Figure 4A). *NIP5;1* mRNA accumulation in roots was more than sevenfold higher under low-B conditions than that under high-B conditions, as reported previously (Takano et al., 2006) (Figure 4B). These experiments were repeated three times, and similar results were obtained in each case. The data show that *NIP5;1* and *NIP6;1* are expressed with different tissue specificity and are both upregulated by B limitation, although to a different extent.

Tissue Specificity of *NIP6;1* Expression

To analyze the tissue and cell specificities of the expression of *NIP6;1*, a 2.3-kb promoter fragment upstream of the transcriptional start site fused to the β-glucuronidase (GUS) reporter gene was introduced into *Arabidopsis* plants. Three independent T3 *Pro-NIP6;1-GUS* transgenic lines were observed, and representative images are shown in Figure 5. Strong GUS staining was observed in nodal regions, the base of flowers, and the petioles of immature young rosette leaves, but no staining was observed in mature leaves (Figures 5A and 5B). The expression patterns were identical under both high and low B supply. In transverse cross sections of petioles and nodes, GUS staining was observed in vascular bundles (Figures 5C to 5F).

To further investigate the cell specificity of *NIP6;1* expression, an expression construct (*Pro-NIP6;1-GFP-NIP6;1*) consisting of a cDNA encoding a NIP6;1-GFP fusion protein driven by the promoter *NIP6;1* was introduced into *Arabidopsis* plants. The GFP fluorescence signal was analyzed in 10 independent T1 transgenic lines, with representative images shown in Figure 6. Cell walls and nuclei were stained with 10 μg/mL propidium iodide. In the cross section of stems, the fluorescence signal of

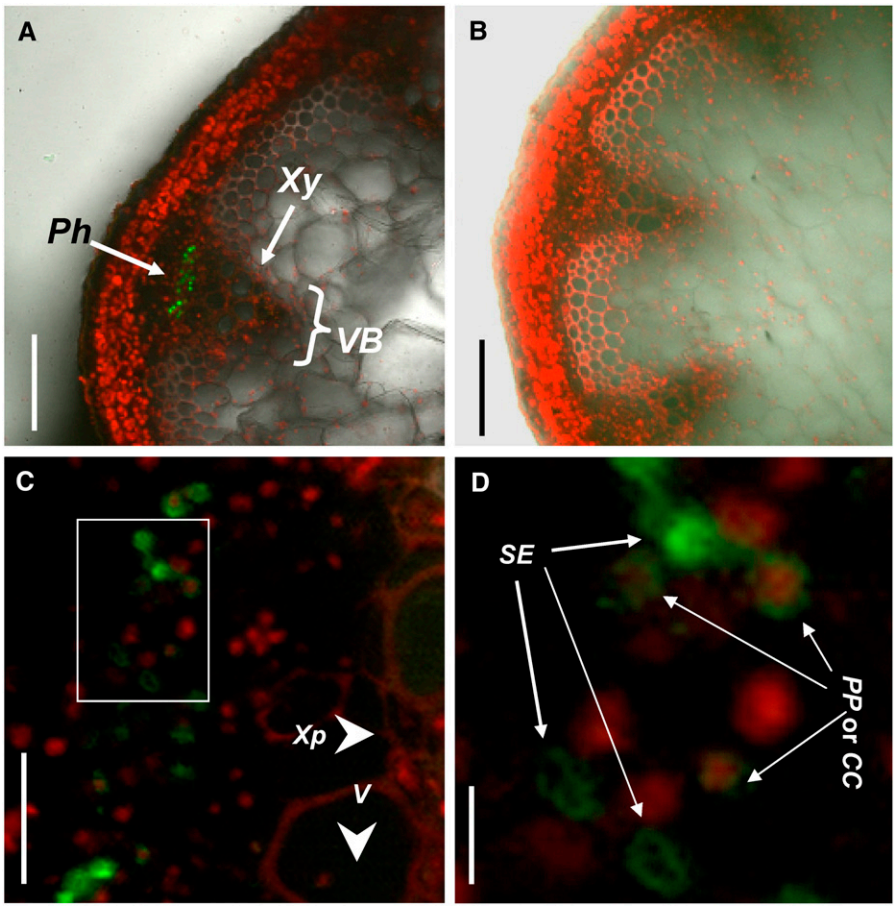

Figure 6. Localization of GFP-NIP6;1 Fusions in Phloem

GFP fluorescence in hand-cut sections of inflorescence stems in *Pro-NIP6;1-GFP-NIP6;1* transgenic plants and Col-0 plants. The stem sections were stained with 10 μg/mL propidium iodide. *Pro-NIP6;1-GFP-NIP6;1* transgenic plants (**[A]**, **[C]**, and **[D]**) and Col-0 plants **(B)** are shown. **(A)** to **(C)** show transverse sections of inflorescence stems in nodal regions, and **(D)** shows a close-up of the vascular strand region (white box) of **(C)**. *CC*, companion cell; *Ph*, phloem; *PP*, phloem parenchyma cell; *SE*, sieve element; *V*, vessel; *VB*, vascular bundle; *Xp*, xylem parenchyma cell; *Xy*, xylem. Bars = 100 μm in **(A)** and **(B)**, 20 μm in **(C)**, and 0.5 μm in **(D)**.

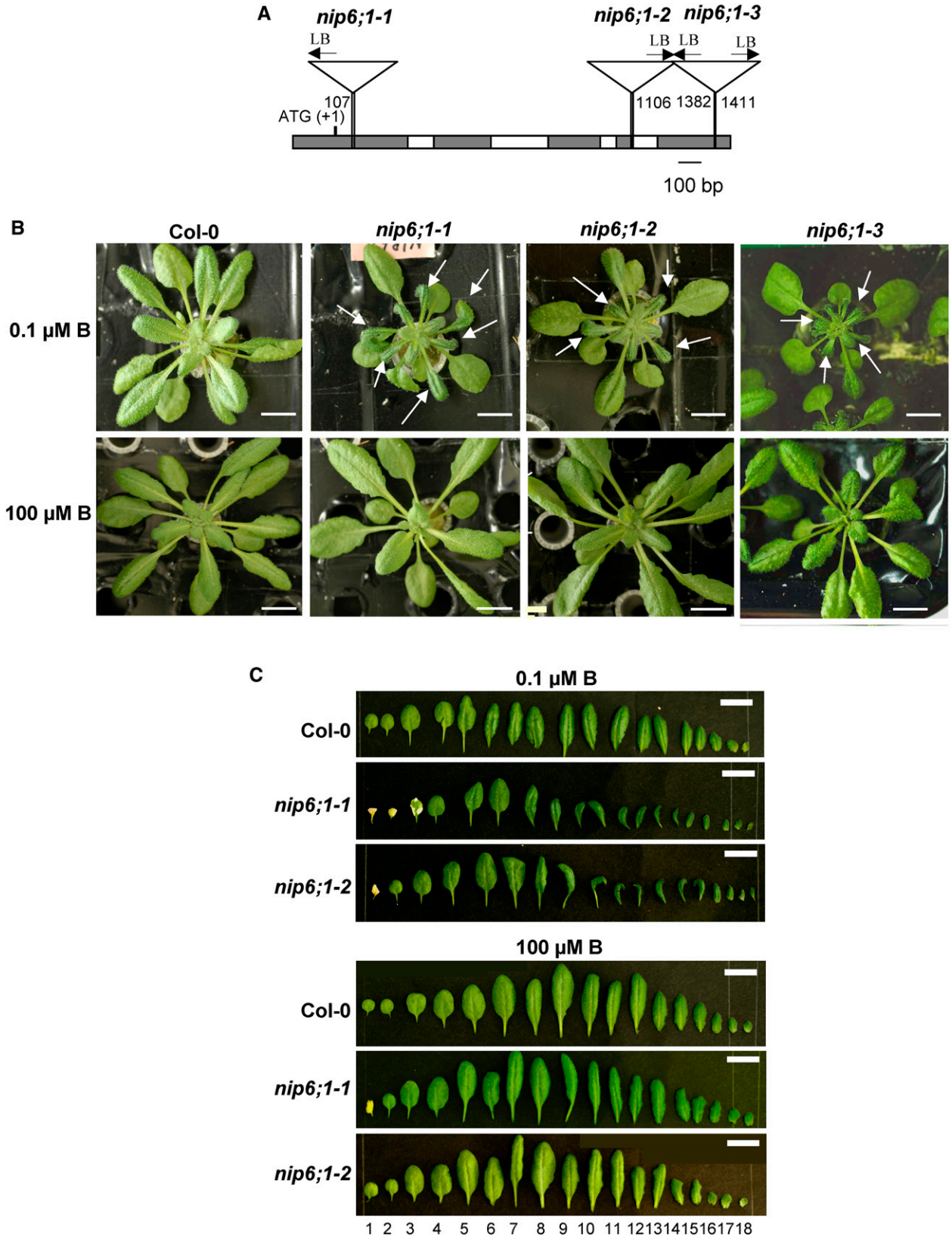

Figure 7. Morphology of Leaves of *NIP6;1* T-DNA Insertion Lines under Normal and Low-B Conditions.

the NIP6;1-GFP fusion protein was most abundant in the region of vascular systems, similar to the case of GUS staining of *Pro-NIP6;1-GUS* transgenic plants (Figures 5D and 6A). No GFP fluorescence was observed in the wild-type Col-0 plants (Figure 6B). High-magnification images of the vascular bundles demonstrated that *NIP6;1* expression is localized on the phloem regions, most likely to the phloem companion cell, phloem parenchyma cell regions, and sieve elements (Figures 6C and 6D). The phloem cells were identified as phloem companion cells and phloem parenchyma cells based on the cells including nuclei and as sieve elements based on the cells including no nuclei.

Plant Growth of *NIP6;1* T-DNA Insertion Mutants

To characterize the function of the *NIP6;1* gene in *Arabidopsis*, three independent T-DNA insertion mutant alleles for *NIP6;1*, SM_3_15719, SALK_046323, and SALK_097969, were obtained and named *nip6;1-1*, *nip6;1-2*, and *nip6;1-3*, respectively. *nip6;1-1* is from the Exon Trapping Insert Consortium, and *nip6;1-2* and *nip6;1-3* are from the SALK Institute. Sequence analysis confirmed T-DNA insertion sites in *nip6;1-1*, *nip6;1-2*, and *nip6;1-3* to be in the first exon, the fourth exon/intron junction, and the 3′ untranslated region of the *NIP6;1* gene, respectively (Figure 7A).

To observe growth patterns, the T-DNA insertion lines were grown hydroponically for 28 d supplied with either a low (0.1 μM) or a high (100 μM) B supply. At late vegetative stages, plants supplied with 0.1 μM B showed small young rosette leaves in all three T-DNA insertion lines compared with Col-0 plants (Figure 7B). The expansion of young rosette leaves was strikingly inhibited in these insertion lines. Young rosette leaves were small and dark green in color and irregular in shape in all three *nip6;1* mutant plants under 0.1 μM B conditions. By contrast, the mature leaves of *nip6;1* mutant plants were apparently normal compared with those of wild-type plants grown under 0.1 μM B conditions (Figures 7B and 7C). These *nip6;1* mutant plants grew in a similar manner to the corresponding wild-type plants under high-B concentrations (100 μM B) (Figures 7B and 7C). Because all three *nip6;1* mutant plants showed a similar phenotype under high- and low-B conditions, *nip6;1-1* and *nip6;1-2* mutant plants were used for further experiments.

At reproductive stages with 1 μM B supply, loss of apical dominance was observed in *nip6;1-1* and *nip6;1-2* mutant plants but not in Col-0 plants (Figure 8). Under 100 μM B supply, *nip6;1-1* and *nip6;1-2* mutant plants showed normal growth with apical dominance (see Supplemental Figure 3 online). These experiments were repeated a minimum of three times, and similar results were obtained in each case. These observations demonstrate that NIP6;1 is required for expansion of young rosette leaves and development of the shoot apices under low-B concentrations.

Anatomical Observation of Rosette Leaves

When wild-type plants were grown under 0.03 μM B, cell sizes of cauline leaves were reduced and the intercellular air spaces were mostly lost in *Arabidopsis* (Takano et al., 2001). To determine whether *nip6;1* mutant plants show a similar developmental defect at low B supply, plants were grown in 1 μM B and the morphology of the young rosette leaves was analyzed (Figure 9). Sections of young rosette leaves of Col-0 plants showed expanded mesophyll cells and well-developed intercellular air spaces (Figure 9A), whereas young rosette leaves from *nip6;1-1* mutant plants showed a smaller cell size and the absence of intercellular air spaces compared with Col-0 plants (Figure 9B). By contrast, both Col-0 plants and *nip6;1-1* mutant plants showed well-expanded mesophyll cells and developed intercellular air spaces in old rosette leaves (Figures 9C and 9D). These experiments were repeated two times, and similar results were obtained in each case. These findings suggest that cell expansion in young rosette leaves was inhibited in *nip6;1-1* mutant plants under low-B conditions.

B Concentrations in *NIP6;1* T-DNA Insertion Mutants

To further examine the function of NIP6;1 in B transport, the B contents of mutant and wild-type plants grown under high- and low-B concentrations were determined using ICP-MS. Young and old rosette leaves or stems with shoot apices and rosette leaves were collected from three to four independent plants at vegetative and reproductive stages, respectively. At late vegetative stages, B concentrations in young rosette leaves of *nip6;1-1* and *nip6;1-2* mutant plants were significantly reduced (26 and 20%, respectively) compared with those of the corresponding leaves in Col-0 plants under low-B growth conditions (5 μM), whereas the B concentrations in the old rosette leaves were not different between the wild type and the insertion lines (Figure 10A). Under high-B (100 μM) growth conditions, there were no significant differences between B concentrations in young and old rosette leaves of wild-type and *nip6;1* mutant plants (Figure 10B).

B concentrations were also measured in stems with shoot apices and rosette leaves during the reproductive stages, and

Figure 7. (continued).

(A) Position of T-DNA insertions of *NIP6;1*. Schematic representation of T-DNA insertion in the *NIP6;1* gene (*nip6;1-1*, *nip6;1-2*, and *nip6;1-3*) is shown. To determine the T-DNA flanking sequences of three *Arabidopsis* T-DNA insertion lines, PCR products with genome-specific primers and T-DNA border primers were sequenced using left borders (LB). Gray and white boxes represent exons and introns, respectively. The numbers shown at the left borders correspond to the relative nucleotide positions from the initiation codon (+1) in the genomic sequence.

(B) and **(C)** Plant growth of *NIP6;1* T-DNA insertion lines.

(B) Wild-type plants and the *NIP6;1* T-DNA insertion lines were grown hydroponically for 28 d supplied with 0.1 and 100 μM B under short-day conditions. Wild-type, *nip6;1-1*, *nip6;1-2*, and *nip6;1-3* plants are shown. Arrows indicate defective young rosette leaves with a reduced size relative to the wild type. Bars = 10 mm.

(C) Rosette leaves were aligned according to leaf number. Bars = 10 mm.

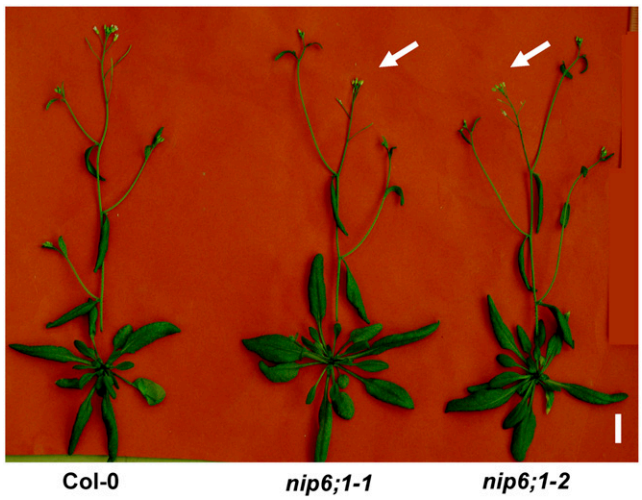

Figure 8. Loss of Apical Dominance in *NIP6;1* T-DNA Insertion Lines under Low-B Growth Conditions at Reproductive Stages.

Wild-type plants and the *NIP6;1* T-DNA insertion lines were grown hydroponically for 28 d supplied with 1 μM B under long-day conditions. Arrows indicate the flowers of the main stem, suggesting the loss of apical dominance. Bar = 10 mm.

the results were similar to those observed at the vegetative stages (Figure 10C). B concentrations in the stems with shoot apices of *nip6;1-1* and *nip6;1-2* mutant plants were significantly reduced (~20% in both lines) compared with those of the corresponding stems with shoot apices in Col-0 plants under low-B growth conditions (1 μM B) (Figure 10C). Under growth conditions of high B (100 μM B), there were no significant differences between B concentrations in stems with shoot apices of wild-type and *nip6;1* mutant plants (Figure 10D). The B concentrations of rosette leaves of mutant and wild-type plants were indistinguishable, regardless of whether plants were grown in low (Figure 10C) or high (Figure 10D) concentrations. These experiments were repeated three times, and similar results were obtained in each case. These data suggest that NIP6;1 is involved in preferential B transport to sink tissues of shoots (e.g., young rosette leaves) under the limiting B conditions.

B Distribution in Various Tissues in *NIP6;1* T-DNA Insertion Mutants

To analyze short-term B uptake and transport, a tracer analysis was done using stable isotopes of B (^{10}B). Wild-type plants and the *NIP6;1* T-DNA insertion lines were precultured for 19 d under long-day conditions with solid medium containing 10 μM B enriched with ^{11}B (99%) until bolting and were transferred to hydroponic culture solution containing 10 μM B enriched with ^{11}B for 9 d. Plants were then treated with medium containing 1 μM B enriched with ^{11}B for an additional 24-h period. At this point, the plants were incubated for 24 h in medium containing either 0.3 or 100 μM B enriched with ^{10}B (99%). Plants were divided into four parts (shoot apices, stems without shoot apices, rosette leaves, and roots), and the ^{10}B contents of each part were determined by ICP-MS.

In plants supplied with 0.3 μM ^{10}B, ^{10}B uptake into shoot apices was reduced by 27% in *nip6;1* mutant plants compared with Col-0 plants (Figure 11A). By contrast, ^{10}B uptake into rosette leaves was slightly higher in *nip6;1-1* mutant plants compared with Col-0 plants. In plants supplied with 100 μM ^{10}B, there was no significant difference in ^{10}B uptake into shoot apices between *nip6;1* mutant plants and Col-0 plants (Figure 11B). ^{10}B uptake into rosette leaves was slightly higher in *nip6;1-1* mutant plants compared with Col-0 plants at 100 μM ^{10}B supply. These experiments were repeated three times, and similar results were obtained in each case. These findings indicate that B transport into shoot apices is disrupted in *nip6;1* mutant plants and provide further support that NIP6;1 is required for preferential B transport to sink tissues of shoots under the conditions of B limitation.

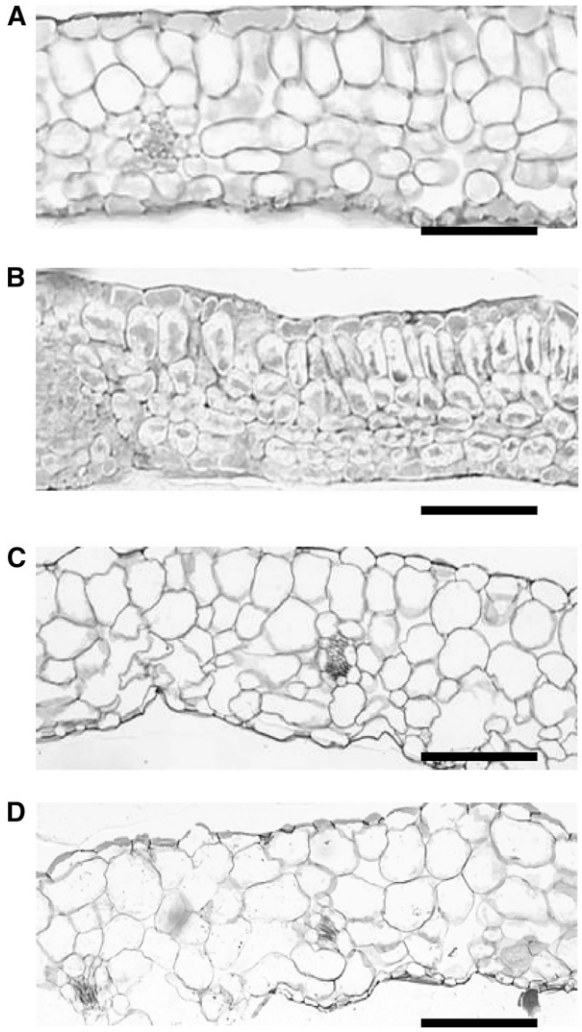

Figure 9. Cross Sections of *nip6;1-1* Rosette Leaves.

Wild-type plants (**[A]** and **[C]**) and the *NIP6;1* T-DNA insertion line (**[B]** and **[D]**) were grown hydroponically for 28 d supplied with 1 μM B. **(A)** and **(B)** show cross sections of young rosette leaves, and **(C)** and **(D)** show cross sections of old rosette leaves. Bars = 50 μm.

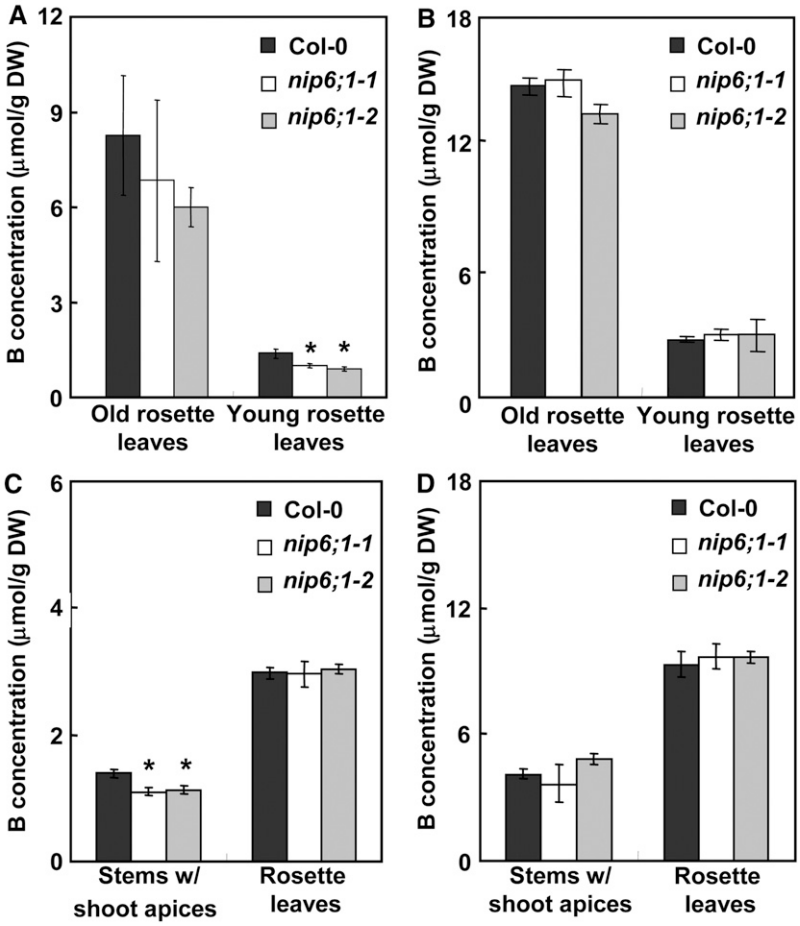

Figure 10. Measurement of the B Contents of Sink Tissues in Shoots in *NIP6;1* T-DNA Insertion Lines under Conditions of B Limitation.

Wild-type plants and the *NIP6;1* T-DNA insertion lines were grown hydroponically under 5 μM B **(A)**, 1 μM B **(C)**, and 100 μM B conditions (**[B]** and **[D]**) for 28 d. Young and old rosette leaves were harvested from short-day-grown plants (**[A]** and **[B]**), and stems with shoot apices and rosette leaves were harvested from long-day-grown plants (**[C]** and **[D]**). At the time of harvest, short-day plants had entered the vegetative stages, while long-day plants were at the reproductive stages. B contents were determined using ICP-MS. Means of three to four biological replicates ± SE are shown. Asterisks denote significant differences from Col-0 plants ($P < 0.05$ by Student's *t* test). DW, dry weight.

DISCUSSION

In this study, we demonstrated that NIP6;1 functions as a plasma membrane boric acid channel required for preferential B transport to sink tissues of shoots under B deficiency. NIP5;1 is a boric acid channel required for B uptake in roots and normal growth of *Arabidopsis* under conditions of B limitation (Takano et al., 2006). NIP6;1 is a similar protein to NIP5;1, but NIP6;1 has different physiological roles in B transport from NIP5;1 in *Arabidopsis*.

NIP6;1 Has Different Transport Properties from NIP5;1 and Forms a Water-Tight Boric Acid Transporter in *Xenopus* Oocytes

NIP6;1 is 66.4% identical in amino acid sequence to NIP5;1 and has identical amino acids composing its selectivity filter, and both are members of the NIP II class of nodulin 26–like intrinsic proteins in *Arabidopsis* (Wallace et al., 2006). Both NIP5;1 and NIP6;1 have a conserved Ala at the H2 position of the ar/R region, compared with Trp, which is a highly conserved residue at this position in NIP subgroup I proteins. According to homology modeling, this substitution generates a much wider pore at the ar/R region in NIP5;1 and NIP6;1 than that in NIP subgroup I (Wallace and Roberts, 2004). Consistent with this observation, NIP6;1 transports larger solutes than the prototypical NIP subgroup I protein, NOD26 (Wallace and Roberts, 2005).

Heterologous expression of NIP6;1 in oocytes shows that, similar to NIP5;1, it facilitates rapid uptake of boric acid across the oocyte plasmalemma. Similar to previous observations with other NIP proteins, boric acid transport shows the properties of channel-based facilitated flux (Figure 1), including inhibition by mercurial compounds (see Supplemental Figure 1 online). Subcellular localization analysis of NIP6;1 using transgenic plants showed localization to the plasma membrane (Figure 3). Taken together, the localization and transport data indicate that NIP6;1 is a plasma membrane boric acid channel in plant cells.

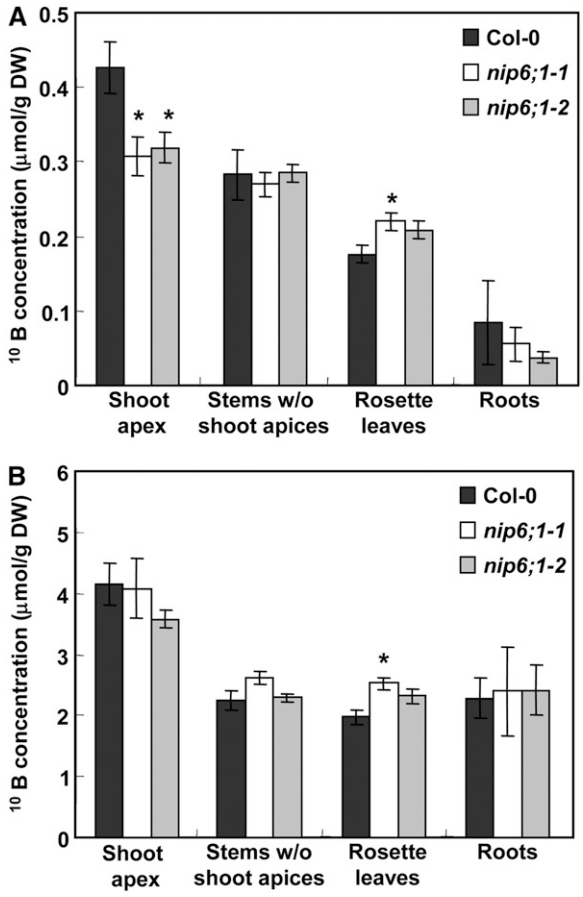

Figure 11. Reduced Translocation of B to Shoot Apices in *NIP6;1* T-DNA Insertion Lines under Conditions of B Limitation at Reproductive Stages.

Wild-type plants and the *NIP6;1* T-DNA insertion lines were grown with medium containing 10 μM B enriched with ^{11}B for 28 d and then transferred to medium containing 1 μM B enriched with ^{11}B for an additional 24-h period. At this point, the plants were incubated for 24 h in medium containing 0.3 or 100 μM B enriched with ^{10}B. **(A)** shows 0.3 μM B and **(B)** shows 100 μM B results. The uptake in 24 h of the tracer B (^{10}B) in shoot apices (the uppermost 1 cm of the stem), stems without shoot apices, rosette leaves, and roots were determined by ICP-MS. Means of three to five biological replicates ± SE (n = 3 to 5) are shown. Asterisks show significant differences from Col-0 plants ($P < 0.05$ by Student's t test). Note that similar experiments were repeated two more times and that the ^{10}B concentrations in rosette leaves of both mutants are 10 to 15% higher than in wild-type plants, although in this particular set of experiments a significant difference was observed in *nip6;1-1* but not in *nip6;1-2*. DW, dry weight.

Similar to previous reports, analyses in this study show that NIP6;1 is completely impermeable to water (Wallace and Roberts, 2005). By contrast, NIP5;1 has measurable water permeability but has a significantly lower P_f compared with PIP2;1, which is known to be an efficient water channel (Takano et al., 2006). The size of the pore in the ar/R region is predicted to be wide enough to simultaneously transport two water molecules in NIP5;1 and NIP6;1 (Wallace and Roberts, 2004). Since both proteins have low water permeability, this suggests that selectivity for water is not solely a function of size selectivity at the ar/R region and that some other mechanisms might contribute to the regulation of water transport activity in NIP5;1 and NIP6;1. Recent structural analyses of aquaporins with low intrinsic water permeabilities show that regions outside of the classical ar/R motif can contribute to gating or restriction of water permeabilities (Hedfalk et al., 2006). Similar structural comparisons of NIP5;1 and NIP6;1 will be necessary to resolve the reason for their low intrinsic water transport rates.

From the point of view of their different roles in plant physiology, it is reasonable that NIP5;1 transports water as well as boric acid whereas NIP6;1 facilitates B transport but is water-impermeable. In the case of *NIP5;1*, expression occurs mainly at the root elongation zone involved in B transport from the root surface into the xylem, along with the pathway of water flow. Thus, in the case of B transport through NIP5;1, it is not necessary to restrict water transport.

In contrast with *NIP5;1*, *NIP6;1* promoter activity was observed between xylem and phloem cells at petioles and nodal regions (Figure 5). In nodal regions, GFP-NIP6;1 was observed in phloem regions, including sieve element, phloem parenchyma cells, and companion cells (Figure 6). This localization pattern suggests that NIP6;1 is involved in xylem–phloem transfer of B. If this is the case, NIP6;1 may need to be water-tight because having water-permeable channels in this cell type may disrupt phloem transport.

NIP6;1 Exhibits Different Tissue-Specific and B-Dependent Expression Patterns from NIP5;1 in *Arabidopsis*

NIP6;1 is also distinct from *NIP5;1* in terms of tissue-specific and B-dependent expression patterns. NIP6;1 expression is mainly in nodal regions and is slightly induced under conditions of B limitation, whereas *NIP5;1* is highly induced in roots under conditions of B limitation (Figures 4 and 5). *NIP6;1* might be regulated in response to internal B concentrations, such as xylem B concentrations for B distribution into shoots. Because B is indispensable for elongation of cell walls and expansion in immature rosette leaves, *NIP6;1* should be constantly expressed to transport sufficient B to sink tissues for normal growth, whereas NIP5;1 must be tightly regulated at transcriptional levels to control B transport into roots.

GUS staining in 10-d-old *Pro-NIP6;1-GUS* seedlings was observed in the first nodes and petioles and veins of all leaves (see Supplemental Figure 4 online), while GUS staining in the plants grown for 28 d was observed in the base of flowers and siliques, nodal regions, and veins and petioles of only young rosette leaves (Figure 5). GUS staining in the petioles and veins of young rosette leaves disappeared along with leaf growth, while GUS staining in nodal regions continued to be detected. As we discuss below, these development-dependent expression profiles suggest roles of NIP6;1 in B distribution within young rosette leaves.

NIP6;1 Plays Important Roles in Preferential Transport of B to Sink Tissues for Normal Growth under Conditions of B Limitation in *Arabidopsis*

Symptoms of B deficiency are in general observed in young tissues (e.g., the root cell elongation and young leaf expansion are inhibited). The main cause of the defective growth is impaired

cell elongation (reviewed in Dell and Huang, 1997). Under low-B conditions, root elongation of *NIP5;1* T-DNA insertion plants is severely inhibited (Takano et al., 2006). In this study, a similar tendency was observed in the defective growth of young rosette leaves in *nip6;1-1* mutant plants under low-B conditions (Figure 9B). Reduced cell size and the absence of intercellular air spaces were observed in young rosette leaves under low-B conditions. This result suggests that the defective growth of young rosette leaves in *nip6;1* mutant plants is due to inhibition of cell elongation rather than to inhibition of cell division.

While expansion of young rosette leaves was inhibited under conditions of B limitation in *nip6;1* mutant plants (Figures 7B and 7C), this inhibition was only observed at certain stages of vegetative growth. For example, during the first and second weeks, the growth of *nip6;1* mutant plants was apparently normal under low-B conditions (see Supplemental Figure 5 online). Even if facilitated uptake of B is disrupted in *nip6;1* mutant plants under low-B conditions (Figure 11A), a smaller but sufficient amount of B molecules might still be taken up into developing tissues by passive diffusion across the lipid bilayer of the cell membrane and other channel proteins. By contrast, the growth of young rosette leaves emerging after several weeks was retarded in *nip6;1* mutant plants under low-B conditions (Figure 7). In the presence of fully expanded leaves that can take up large amounts of B through high transpiration rate, facilitated transport of B through NIP6;1 seems to be required to provide enough B for young rosette leaves.

Tracer experiments demonstrated that short-term ^{10}B uptake into shoot apices is lower in *nip6;1* mutant plants than in the wild-type plants under low-B conditions but not under high-B conditions (Figure 11), suggesting that B is not distributed efficiently to sink tissues in *nip6;1* mutant plants. These findings indicate that NIP6;1 is crucial for preferential distribution of B to sink tissues in shoots.

Possible Involvement of NIP6;1 in Xylem–Phloem Transfer under Low-B Conditions

In *Arabidopsis*, BOR1, a B efflux transporter, is involved not only in xylem loading of B in roots but also in the distribution of B to

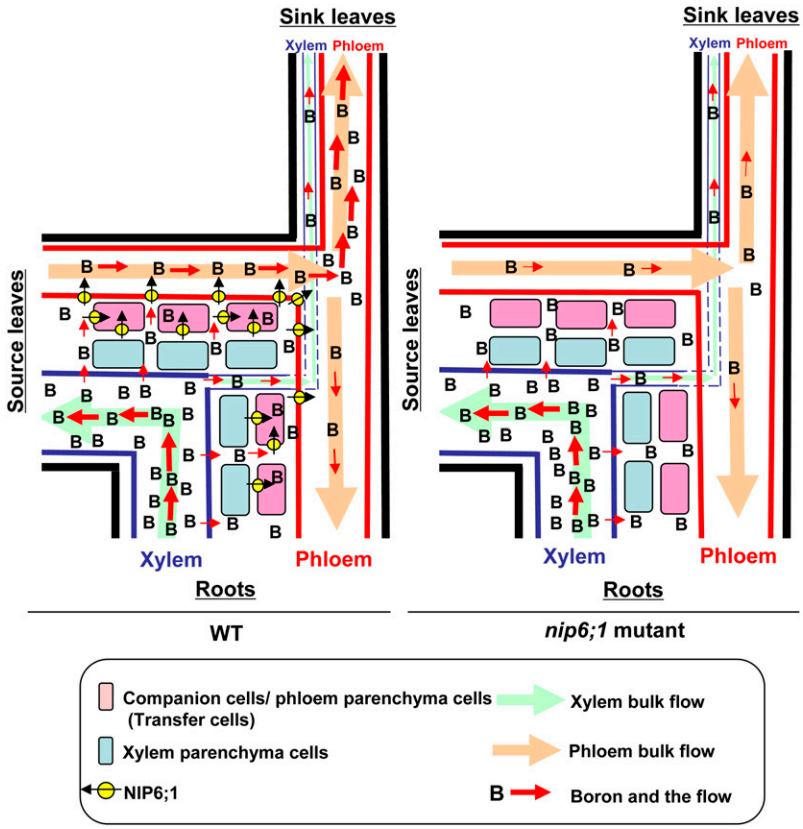

Figure 12. Model for the Roles of NIP6;1 in the Nodal Region in B Transport in *Arabidopsis*.

The schematic diagram shows B flow in nodal regions. Cell profiles between xylem and phloem are simplified and grouped into two cell types. Pink boxes show cells in which NIP6;1 is expressed, including companion and phloem parenchyma cells, while blue boxes show cells in which NIP6;1 is not expressed, including xylem parenchyma cells. In this diagram, B transport from/to roots, source leaves, and sink leaves through xylem and phloem were compared between wild-type (left) and *nip6;1* mutant (right) plants. In the wild type, B transported from roots to nodal regions via xylem is unloaded and B is transferred across companion and phloem parenchyma cells to phloem through NIP6;1. By contrast, in the *nip6;1* mutant, B transported to nodal regions is unloaded from the xylem, as is the case in wild-type plants, but B is transferred to phloem without facilitated transport by NIP6;1 and results in reduced B transport to sink organs.

young rosette leaves. *bor1-1* mutant plants showed growth reduction in young rosette leaves under conditions of B limitation (Noguchi et al., 1997; Takano et al., 2001). A tracer experiment showed that higher amounts of B were transported to young rosette leaves compared with old rosette leaves only under low-B supply in wild-type plants but not in *bor1-1* mutant plants, suggesting that B is preferentially transported to young tissues via BOR1 under low-B conditions (Takano et al., 2001). In roots, NIP5;1 is involved in acquisition of B and is expressed in root epidermal, cortical, and endodermal cells, while BOR1 is involved in xylem loading and is expressed in stelar cells. Similarly, transport of B through NIP6;1 and BOR1 at different steps may be required for partitioning of B to young rosette leaves.

In this study, we provide the following evidence that supports a role of NIP6;1 in the xylem–phloem transfer of B. First, NIP6;1 is expressed in branching points (stem nodal regions) and junction areas (the base of flowers and siliques) (Figure 5), known as places for rapid xylem–phloem transfer (reviewed in Marschner, 1995; Offler et al., 2002; Royo et al., 2007). Second, NIP6;1 is a plasma membrane protein that has a robust B permeability but no water permeability. Third, in the *nip6;1* mutant plants, the defective growth is only observed in sink tissues such as young rosette leaves and the shoot apices. Fourth, the transport and accumulation of B in young rosette leaves and the shoot apices were significantly decreased under low-B conditions. These observations support the hypothesis that NIP6;1 is involved in preferential B transport to sink tissues in shoots via xylem–phloem transfer. In Figure 12, we propose a model for the roles of NIP6;1 in xylem–phloem transfer of B in the nodal regions. In this simplified diagram, cells present between xylem and phloem are grouped into two types, companion cells/phloem parenchyma cells and xylem parenchyma cells. In Col-0, NIP6;1 expressed in companion cells/phloem parenchyma cells and phloem cells facilitate the rapid diffusion of boric acid toward phloem, while in the *nip6;1* mutants, this diffusion process is slow. The companion cells/phloem parenchyma cells expressing NIP6;1 (Figure 6) might include transfer cells, a specialized type of parenchyma cells for xylem–phloem transfer (Offler et al., 2002; Royo et al., 2007).

Our observations also suggest other roles of NIP6;1. *NIP6;1* is expressed strongly in young rosette leaves compared with old rosette leaves (Figure 5; see Supplemental Figure 4 online). Expression in veins of young rosette leaves is not likely to be involved in xylem–phloem transfer of B, as such a process in these tissues is likely to be minimal. NIP6;1 in these tissues may rather be involved in unloading of B from phloem and xylem to facilitate B diffusion to developing leaf mesophyll cells.

Evolutionary and Functional Relationship between NIP5;1, NIP6;1, and Rice NIP3;1

Unlike *Arabidopsis*, which has two closely related B-transporting NIPs (NIP5;1 and NIP6;1), rice (*Oryza sativa*) has only one gene, Os *NIP3;1*, that is highly similar to *NIP5;1* and *NIP6;1* (Wallace et al., 2006). Os NIP3;1 is localized on the plasma membrane and is regulated by B availability, as is the case of NIP5;1. However, tissue localization of Os NIP3;1 showed that it is involved in both B uptake in roots and B transport to shoots (Hanaoka and Fujiwara, 2007). This expression pattern of Os *NIP3;1* seems to be a combined pattern of both *NIP5;1* and *NIP6;1*. During the evolution of *Arabidopsis*, NIP5;1 and NIP6;1 apparently became diversified in terms of both tissue specificity of expression and water permeation properties, while maintaining their B transport activities and their ability to be induced under low-B conditions.

In this study, we demonstrated that NIP6;1 is a boric acid channel involved in preferential B transport to growing tissues of plants and showed the function of a boric acid channel in shoots in *Arabidopsis*. Transport of B to growing tissues of plants under B-deficient conditions occurs not only by apoplastic flow via the transpiration stream but also via other mechanisms, such as xylem–phloem transfer, which involve facilitated flux across the membranes of living cells. NIP6;1 is involved in this latter mechanism.

METHODS

Plant Materials

Col-0 of *Arabidopsis thaliana* was derived from our laboratory stocks. Information about the T-DNA insertion lines was obtained from the SIGnAL database (Alonso et al., 2003), and the seeds were obtained from the ABRC. The genotypes of plants were determined by PCR using the left border T-DNA–specific primer LBa1 (5′-TGGTTCACGTAGTGGCCATCG-3′) and the gene-specific primers *nip6;1-1* (5′-TTCCAAATTTTATAAGCATCGTCG-3′), *nip6;1-2* (5′-CCCACTTACTCCTCACTCCAACC-3′), and *nip6;1-3* (5′-TTCCAAATTTTATAAGCATCGTCG-3′ and 5′-ATCCGGCTGTAACCATTGCCT-3′).

Plant Growth Conditions

For phenotypic analysis and the determination of B concentration, plants were grown with hydroponic culture (Fujiwara et al., 1992) at 22°C in a growth chamber, and concentrations of B in the medium were adjusted by adding boric acid without affecting pH. To observe vegetative and reproductive growth, plants were grown under short-day conditions (10-h/14-h light/dark cycle) and long-day conditions (16-h/8-h light/dark cycle), respectively. The growth conditions for hydroponic cultures were described previously (Takano et al., 2001). For the tracer experiment of B uptake using stable isotopes of B, plants were grown as described by Takano et al. (2005). For confocal imaging experiments, plants were grown in solid medium containing 1% (w/v) sucrose and 1.5% (w/v) gellan gum. Surface-sterilized seeds were sown on the plates and incubated for 1 to 2 d at 4°C, and the plates were placed vertically for 10 d at 22°C in a growth chamber under long-day conditions.

Expression of NIP6;1 and NIP5;1 in *Xenopus* Oocytes

Xenopus laevis expression constructs of NIP6;1 (Wallace and Roberts, 2005) and NIP5;1 (Takano et al., 2006) were prepared in the pXβG-ev-1 vector with an in-frame N-terminal FLAG epitope tag as described previously (Wallace and Roberts, 2005; Takano et al., 2006). Capped cRNA was transcribed from the plasmids in vitro using the mMessage mMachine kit (Ambion) after linearization of the plasmid with *Xba*I. *Xenopus* oocytes (stages V and VI) were surgically removed from adult female frogs, defolliculated, and cultured as described previously (Rivers et al., 1997; Dean et al., 1999). Oocytes were injected with 46 ng of cRNA (1 ng/nL) and incubated at 16°C for 72 h in Ringer's solution (96 mM NaCl, 2 mM KCl, 5 mM $MgCl_2$, 0.6 mM $CaCl_2$, and 5 mM HEPES, pH 7.5; osomolarity = 190 mosmol/kg). Either uninjected oocytes or mock-injected oocytes to which 46 nL of sterile water was injected were used

as negative controls for transport assays. All cRNA-injected oocytes and control oocytes were viable and recovered normal membrane integrity and showed plasma membrane resting potentials (−25 to −35 mV) indistinguishable from those of uninjected control oocytes measured as described previously (Vincill et al., 2005).

Osmotic swelling assays for boric acid uptake were conducted by placing the oocytes in isoosmotic Ringer's solution (190 mosmol/kg) with the transport solute (200 mM boric acid) replacing NaCl. The P_f of oocytes was measured at 15°C from the rate of oocyte swelling in hypoosmotic medium (30% Ringer's solution) as described previously (Wallace and Roberts, 2005). Mercury treatment was conducted by placing the oocytes in Ringer's solution containing 1 mM $HgCl_2$ at 25°C for 5 min. The swelling of oocytes was monitored with video microscopy imaging, and the rate of swelling was calculated as described previously (Wallace and Roberts, 2005).

The relative expression of NIP5;1 and NIP6;1 in oocytes was assayed by protein gel blot analyses of *Xenopus* oocyte lysates with an anti-FLAG antibody as described previously (Wallace and Roberts, 2005).

Direct B Uptake Measurement in *Xenopus* Oocytes

Direct boric acid uptake was performed by incubating oocytes in Ringer's solution (96 mM NaCl, 2 mM KCl, 5 mM $MgCl_2$, 0.6 mM $CaCl_2$, and 5 mM HEPES NaOH, pH 7.5; osomolarity = 190 mosmol/kg) containing 2 mM boric acid at 15°C. Oocyte samples were removed at 0, 5, 10, and 20 min and were washed three times with 30 mL of ice-cold Ringer's solution without boric acid, then they were separated into batches of four oocytes and lyophilized. The oocytes were digested with concentrated nitric acid, and the B contents were determined using ICP-MS (SPQ-9000; Seiko Instruments) as described previously (Takano et al., 2001).

Expression of GFP-Tagged NIP6;1 in *Arabidopsis* Seedlings

A plasmid carrying the cauliflower mosaic virus 35S RNA promoter (*P35S*)-*NIP6;1* was constructed as follows. The *NIP6;1* cDNA clone was amplified from *Arabidopsis* Col-0 genomic DNA by PCR using primers 5′-CCTCGCATGGATCATGAGG-3′ and 5′-TAATATAGAAGCGAGTGT-TTTTC-3′. The amplified fragment was A-tailed and cloned into the pGEM-T Easy vector according to the manufacturer's instructions (Promega). Accuracy of the cloned PCR product was confirmed by DNA sequencing. The *NIP6;1* cDNA clone was then amplified from the above plasmid by PCR using primers 5′-CACCGATCATGAGGAAATTC-CATCCAC-3′ and 5′-TCATCTTCTGAAGCTCCTCCTCTCT-3′. The forward primer contains CACC at the 5′ end for TOPO cloning as underlined. The amplified fragment was subcloned into the pENTR/D-TOPO vector via the TOPO cloning reaction (Gateway Technology; Invitrogen). The cloned promoter fragment was subsequently subcloned into pMDC43 (Curtis and Grossniklaus, 2003), which contains the dual P35S, the synthetic mutant green fluorescent protein (sGFP; S65T), and the transcriptional terminator of the gene for nopaline synthase (Nos T). Cloning was performed using the Gateway system by LR recombination reaction, to T-DNA fragments from entry clones to destination vectors, according to the manufacturer's instructions (Invitrogen).

A plasmid carrying *promoter NIP5;1-GFP* was constructed as follows. The region from −2188 to +312 was amplified from BAC clone F24G24 obtained from the ABRC by PCR using primers 5′-GGTGGATCCGAAAG-CAAGCATTCCCTG-3′ and 5′-GAGCCATGGCCAACGTTTTTTTTTTT-GGT-3′. *Bam*HI and *Nco*I recognition sites are underlined, respectively. The 5′ end of full-length cDNA (The Arabidopsis Information Resource database) was used as the predicted transcript start site (+1). The region from −2188 to +312 was excised from the clone using *Bam*HI and *Nco*I, and the fragment was subcloned into pTF441. pTF441 was constructed from pBI221 (Jefferson et al., 1987) and contains a modified *GFP* open reading frame with an extra ATGGTA sequence at the 5′ end of the original *GFP* open reading frame to generate a *Nco*I site. The *Bam*HI–*Nco*I fragment from the plasmid was subcloned into the *Bam*HI–*Bsp*120-I vector fragment from the binary vector pTkan$^+$ (Takano et al., 2006). The resulting plasmid was termed *Pro-NIP5;1-GFP*, as described in Results.

Arabidopsis Col-0 plants were transformed using the floral-dip method (Clough and Bent, 1998). *35S-GFP-NIP6;1* and *Pro-NIP5;1-GFP* transgenic *Arabidopsis* plants (homozygous T3) were grown for 10 d on vertically placed solid medium containing 100 and 0.3 μM B. For the staining of tonoplasts, plants were incubated with 20 μM FM4-64 (Molecular Probes) for 5 min, washed three times in water, and incubated on the solid medium for 18 h under dark conditions. For the staining of cell walls, roots were incubated in 10 μg/mL propidium iodide (Molecular Probes) before applying 0.5 M mannitol solution. Plates were scanned with excitation at 488 nm (argon laser) and detection with a 515- to 545-nm filter (green; GFP fluorescence), a >560-nm filter (red; FM4-64), and a 610-nm filter (red; propidium iodide fluorescence) by confocal laser scanning microscope (FLUOVIEW500; Olympus). Differential interference contrast images were also obtained with Nomarski optics.

Quantification of Transcript Accumulation by RT-PCR

Plants were grown under long-day conditions in solid medium supplied with 100 μM B for 29 d and were transferred to hydroponic culture supplied with 100 μM B for 17 d. Plants were then incubated in hydroponic culture solutions containing 0.1 or 100 μM B for 24 h prior to sample collection. Roots, rosette leaves, and stems were separately collected from three independent plants. Total RNA was extracted using the RNeasy Plant Mini kit (Qiagen) as recommended by the manufacturer. Total RNA (500 ng) was reverse-transcribed into cDNA in a 20-μL reaction using the PrimeScript RT reagent kit (Takara) with oligo$(dT)_{16}$ primer for RT-PCR. The cDNA was amplified by PCR in a Thermal Cycler Dice (Takara) with SYBR Premix Ex Taq II (Takara). The *Elongation Factor1-α* (*EF1-α*) gene was used as a control for quantitation. The primers used in RT-PCR were as follows: 5′-GGCAATGGTTACAGCCGGAT-3′ and 5′-GGAGCTGAGACGCTTATTGGTT-3′ for *NIP6;1*; 5′-CACCGATTTTC-CCTCTCCTGAT-3′ and 5′-GCATGCAGCGTTACCGATTA-3′ for *NIP5;1*; and 5′-CCTTGGTGTCAAGCAGATGA-3′ and 5′-TGAAGACACCTCCTT-GATGATTT-3′ for *EF1-α*. Specific amplification of target genes was confirmed both by electrophoresis and by melting curve analysis of PCR products using the Thermal Cycler Dice instrument. The relative expression levels of *NIP6;1* and *NIP5;1* were calculated using the standard curve method and standardized using *EF1-α* as a calibrator.

Histochemical Analysis of NIP6;1

The 2355-bp promoter region upstream of the initiation codon of *NIP6;1* containing the 5′ untranslated region (+196) was amplified from *Arabidopsis* Col-0 genomic DNA by PCR using primers 5′-CACCTCGAAC-GACGATTAATGGAG-3′ and 5′-GTCGAGGGTAGAGAGATAGATGAG-ATC-3′. The forward primer contains CACC at the 5′ end for TOPO cloning as underlined. The amplified DNA fragment was subcloned into the pENTR/D-TOPO vector via the TOPO cloning reaction (Gateway Technology). The cloned promoter fragment was subsequently subcloned into pMDC162 (Curtis and Grossniklaus, 2003) containing the *GUS* gene using the Gateway system as described previously. The resulting plasmid was termed *Pro-NIP6;1-GUS* as described in Results.

Arabidopsis Col-0 plants were used for plant transformation. The *Pro-NIP6;1-GUS* transgenic plants (homozygous T3) were grown with hydroponic culture solution containing 30 μM B for 28 d under long-day conditions prior to histochemical analysis. GUS staining was performed as described previously (Shibagaki et al., 2002). Cross sections of petioles and stems were prepared as follows. The petioles and stems were fixed in 4% (w/v) paraformaldehyde in microtubule-stabilizing buffer (50 mM PIPES, 5 mM EGTA, and 0.2% [w/v] Triton X-100) for several

hours. Samples were washed with 2% (w/v) sucrose in microtubule-stabilizing buffer (two times, 15 min each), and the petioles and stems were cut into small pieces. The samples were then dehydrated through a graded ethanol series (30, 50, 70, and 80% on ice two times, 10 min each, followed by 90 and 95% at room temperature two times, 10 min each, and then 100% two times, 30 min each) and then were embedded in Technovit 7100 (Heraeus Kulzer), according to the manufacturer's protocol. Sections of 5 μm in thickness were cut with a microtome.

The 2355-bp region upstream of the initiation codon of *NIP6;1* was amplified from *Arabidopsis* Col-0 genomic DNA by PCR using the following primers: 5′-GAGCTGCAGGGATTCAAAGATTATGGGA-3′ and 5′-AATGGTACCGTCGAGGGTAGAGATAGATG-3′. *Pst*I and *Kpn*I recognition sites are underlined, respectively. The amplified region was excised by digestion with *Pst*I and *Kpn*I, and the fragment was subcloned into the *Pst*I–*Kpn*I sites of the binary vector, *35S-GFP-NIP6;1*, containing the *GFP-NIP6;1* fragment. The resulting plasmid was termed *Pro-NIP6;1-GFP-NIP6;1* as described in Results. The construct was introduced into *Arabidopsis* plants, and T1 transgenic plants were grown with rockwool and vermiculite for 5 to 6 weeks. Sections of inflorescence stems in the nodal regions were cut by hand using a razor blade, incubated in 10 μg/mL propidium iodide, and analyzed by confocal laser scanning microscopy (LSM 510; Carl Zeiss).

Anatomical Observation of Rosette Leaves

Plants were grown hydroponically for 28 d under short-day conditions with 1 μM B and were subjected to anatomical analysis. The 5th leaves from the bottom were harvested (these leaves were referred to as old leaves), while the 16th to 19th leaves from the bottom were also harvested (these leaves were referred to as young rosette leaves). Samples were fixed in 4% (w/v) paraformaldehyde in microtubule-stabilizing buffer and dehydrated through a graded ethanol series, then embedded in Technovit 7100 as described above. Sections of 5 μm in thickness were cut with a microtome and stained with 0.05% (w/v) toluidine blue at 50°C for 30 s.

Measurement of B Content in Plants

Plants were grown with hydroponic culture solutions containing 5 and 100 μM B and 1 and 100 μM B for 28 d under long-day conditions and short-day conditions, respectively. The first and second rosette leaves from the bottom were harvested (these leaves were referred to as old leaves), while the two youngest leaves that were longer than 3 mm were also harvested (these leaves were referred to as young rosette leaves) from three to four independent plants under short-day conditions for the analysis during the vegetative stages. Stems with shoot apices and rosette leaves were harvested from three to four independent plants under long-day conditions for the analysis during the reproductive stages. The B contents of these samples were determined using ICP-MS. For determination of ^{10}B in the tracer experiment, plants were grown on solid medium containing 10 μM B enriched with ^{11}B (99%; Cambridge Isotope Laboratories) for 19 d until bolting of plants and then were transferred to hydroponic culture supplied with 10 μM B enriched with ^{11}B for 9 d. By this time, plants started to flower. Plants were then transferred to hydroponic culture solutions containing 0.1 μM B enriched with ^{11}B for 24 h and were incubated in 0.3 or 100 μM B enriched with ^{10}B (99%; Cambridge Isotope Laboratories) for 0 and 24 h. After 0 and 24 h of incubation, shoot apices (the uppermost 1 cm of the stem), stems without shoot apices, rosette leaves, and roots were separately harvested from three to five independent plants and the ^{10}B contents of these samples were determined using ICP-MS. The data in Figure 11 represent the ^{10}B concentrations taken up during the 24 h of uptake. The values of ^{10}B taken up during 24 h of incubation were calculated by subtracting the mean of ^{10}B concentrations at 0 h from the actual ^{10}B concentrations after 24 h of incubation.

Accession Numbers

Arabidopsis Genome Initiative locus identifiers for NIP6;1 and NIP5;1 are At1g80760 and At4g10380, respectively.

Supplemental Data

The following materials are available in the online version of this article.

Supplemental Figure 1. Comparison of Swelling Rates of Control and NIP Oocytes and Mercury Inhibition of Swelling.

Supplemental Figure 2. FLAG-Tag Protein Gel Blot of *Xenopus* Oocyte Lysates.

Supplemental Figure 3. Plant Growth under High-B Conditions.

Supplemental Figure 4. GUS Staining in *Pro-NIP6;1-GUS* Transgenic Seedlings.

Supplemental Figure 5. Plant Growth of *NIP6;1* T-DNA Insertion Lines for 14 d.

ACKNOWLEDGMENTS

The T-DNA insertion lines were kindly provided by the ABRC at Ohio State University. We thank M. Wada, Y. Kawara, and K. Aizawa for excellent technical assistance and K. Miwa and H. Hanaoka for discussion. This work was supported in part by a Grant-in-Aid for Scientific Research on Priority Areas from the Ministry of Education, Culture, Sports, Science, and Technology of Japan to T.F., by a grant from the Ministry of Agriculture, Forestry, and Fisheries of Japan (Genomics for Agricultural Innovation; Grant IPG-0005) to T.F., and by National Science Foundation Grant MCB-0618075 to D.M.R.

Received February 12, 2008; revised September 26, 2008; accepted October 2, 2008; published October 24, 2008.

REFERENCES

Alonso, J.M., et al. (2003). Genome-wide insertional mutagenesis of *Arabidopsis thaliana*. Science **301:** 653–657.

Brown, P.H., and Hu, H. (1996). Phloem mobility of boron is species dependent. Evidence for phloem mobility in sorbitol rich species. Ann. Bot. (Lond.) **77:** 497–505.

Brown, P.H., and Shelp, B.J. (1997). Boron mobility in plants. Plant Soil **193:** 85–101.

Choi, W.G., and Roberts, D.M. (2007). *Arabidopsis* NIP2;1, a major intrinsic protein transporter of lactic acid induced by anoxic stress. J. Biol. Chem. **282:** 24209–24218.

Clough, S.J., and Bent, A.F. (1998). Floral dip: A simplified method for *Agrobacterium*-mediated transformation of *Arabidopsis thaliana*. Plant J. **16:** 735–743.

Curtis, M., and Grossniklaus, U. (2003). A Gateway cloning vector set for high-throughput functional analysis of genes in plants. Plant Physiol. **133:** 462–469.

Dean, R.M., Rivers, R.L., Zeidel, M.L., and Roberts, D.M. (1999). Purification and functional reconstitution of soybean nodulin 26. An aquaporin with water and glycerol transport properties. Biochemistry **38:** 347–353.

Dell, B., and Huang, L. (1997). Physiological response of plants to low boron. Plant Soil **193:** 103–120.

Dordas, C., Chrispeels, M.J., and Brown, P.H. (2000). Permeability and channel-mediated transport of boric acid across membrane vesicles isolated from squash roots. Plant Physiol. **124:** 1349–1361.

Fort, D.J., Propst, T.L., Stover, E.L., Strong, P.L., and Murray, F.J.

(1998). Adverse reproductive and developmental effects in *Xenopus* from insufficient boron. Biol. Trace Elem. Res. **66:** 237–259.

Fortin, M.G., Morrison, N.A., and Verma, D.P. (1987). Nodulin-26, a peribacteroid membrane nodulin is expressed independently of the development of the peribacteroid compartment. Nucleic Acids Res. **15:** 813–824.

Fujiwara, T., Hirai, M.Y., Chino, M., Komeda, Y., and Naito, S. (1992). Effects of sulfur nutrition on expression of the soybean seed storage protein genes in transgenic petunia. Plant Physiol. **99:** 263–268.

Hanaoka, H., and Fujiwara, T. (2007). Channel-mediated boron transport in rice. Plant Cell Physiol. **48:** S227.

Hedfalk, K., Törnroth-Horsefield, S., Nyblom, M., Johanson, U., Kjellbom, P., and Neutze, R. (2006). Aquaporin gating. Curr. Opin. Struct. Biol. **16:** 447–456.

Huang, L., Bell, W.L., and Dell, B. (2008). Evidence of phloem boron transport in response to interrupted boron supply in white lupin (*Lupinus albus* L. cv. Kiev Mutant) at the reproductive stage. J. Exp. Bot. **59:** 575–583.

Jefferson, R.D., Kavanagh, T.A., and Bevan, M.W. (1987). GUS fusions: β-Glucuronidase as a sensitive and versatile gene fusion marker in higher plants. EMBO J. **6:** 3901–3907.

Johanson, U., Karlsson, M., Johansson, I., Gustavsson, S., Sjovall, S., Fraysee, L., Weig, A.R., and Kjellbom, P. (2001). The complete set of genes encoding major intrinsic proteins in *Arabidopsis* provides a framework for a new nomenclature for major intrinsic proteins in plants. Plant Physiol. **126:** 1358–1369.

Loomis, W.D., and Durst, R.W. (1992). Chemistry and biology of boron. Biofactors **3:** 229–239.

Marschner, H. (1995). Mineral Nutrition of Higher Plants, 2nd ed. (San Diego, CA: Academic Press).

Matoh, T., and Ochiai, K. (2005). Distribution and partitioning of newly take-up boron in sunflower. Plant Soil **278:** 351–360.

Maurel, C. (2007). Plant aquaporins: Novel functions and regulation properties. FEBS Lett. **581:** 2227–2236.

Mizutani, M., Watanabe, S., Nakagawa, T., and Maeshima, M. (2006). Aquaporin NIP2;1 is mainly localized to the ER membrane and shows root-specific accumulation in *Arabidopsis thaliana*. Plant Cell Physiol. **47:** 1420–1426.

Noguchi, K., Dannel, F., Pfeffer, H., Romheld, V., Hayashi, H., and Fujiwara, T. (2000). Defect in root-shoot translocation of boron in *Arabidopsis thaliana* mutant *bor1-1*. J. Plant Physiol. **156:** 751–755.

Noguchi, K., Yasumori, M., Imai, T., Naito, S., Matsunaga, T., Oda, H., Hayashi, H., Chino, M., and Fujiwara, T. (1997). *bor1-1*, an *Arabidopsis thaliana* mutant that requires a high level of boron. Plant Physiol. **115:** 901–906.

Offler, C.E., McCurdy, D.W., Patrick, J.W., and Talbot, M.J. (2002). Transfer cells: Cells specialized for a special purpose. Annu. Rev. Plant Biol. **54:** 431–454.

O'Neill, M.A., Eberhard, S., Albersheim, P., and Darvill, A.G. (2001). Requirement of borate cross-linking of cell wall rhamnogalacturonan II for *Arabidopsis* growth. Science **294:** 846–849.

O'Neill, M.A., Ishii, T., Albersheim, P., and Darvill, A.G. (2004). Rhamnogalacturonan II: Structure and function of a borate cross-linked cell wall pectic polysaccharide. Annu. Rev. Plant Biol. **55:** 109–139.

Raven, J.A. (1980). Short- and long-distance transport of boric acid in plants. New Phytol. **84:** 231–249.

Rivers, R.L., Dean, R.M., Chandy, G., Hall, J.E., Roberts, D.M., and Zeidel, M.L. (1997). Functional analysis of nodulin 26, an aquaporin in soybean root nodule symbiosomes. J. Biol. Chem. **272:** 16256–16261.

Rowe, R.I., and Eckhert, C.D. (1999). Boron is required for zebrafish embryogenesis. J. Exp. Biol. **202:** 1649–1654.

Royo, J., Gomrz, E., and Hueros, G. (2007). Transfer cells. In Endosperm Development and Molecular Biology. Plant Cell Monographs Series, A. Olsen, ed (Berlin: Springer-Verlag), pp. 73–90.

Shelp, B.J., Kitheka, A.M., Vanderpool, R.A., Van Cauwenberghe, O.R., and Spiers, G.A. (1998). Xylem-to-phloem transfer of boron in broccoli and lupin during early reproductive growth. Physiol. Plant. **104:** 533–540.

Shibagaki, N., Rose, A., McDermott, J.P., Fujiwara, T., Hayashi, H., Yoneyama, T., and Davies, J.P. (2002). Selenate-resistant mutants of *Arabidopsis thaliana* identify Sultr1;2, a sulfate transporter required for efficient transport of sulfate into roots. Plant J. **29:** 475–486.

Shorrocks, V.M. (1997). The occurrence and correction of boron deficiency. Plant Soil **193:** 121–148.

Stangoulis, J.C., Brown, P.H., Bellaloui, N., Reid, R.J., and Graham, R.D. (2001a). The efficiency of boron ulitisation in canola. Aust. J. Plant Physiol. **28:** 1109–1114.

Stangoulis, J.C.R., Reid, R.J., Brown, P.H., and Graham, R.D. (2001b). Kinetic analysis of boron transport in *Chara*. Planta **213:** 142–146.

Takano, J., Miwa, K., and Fujiwara, T. (2008). Boron transport mechanisms: Collaboration of channels and transporters. Trends Plant Sci. **13:** 451–457.

Takano, J., Miwa, K., Yuan, L., von Wiren, N., and Fujiwara, T. (2005). Endocytosis and degradation of BOR1, a boron transporter of *Arabidopsis thaliana*, regulated by boron availability. Proc. Natl. Acad. Sci. USA **102:** 12276–12281.

Takano, J., Noguchi, K., Yasumori, M., Kobayashi, M., Gajdos, Z., Miwa, K., Hayashi, H., Yoneyama, T., and Fujiwara, T. (2002). *Arabidopsis* boron transporter for xylem loading. Nature **420:** 337–340.

Takano, J., Wada, M., Ludewig, U., Schaaf, G., von Wiren, N., and Fujiwara, T. (2006). The *Arabidopsis* major intrinsic protein NIP5;1 is essential for efficient boron uptake and plant development under boron limitation. Plant Cell **18:** 1498–1509.

Takano, J., Yamagami, M., Noguchi, K., Hayashi, H., and Fujiwara, T. (2001). Preferential translocation of boron to young rosette leaves in *Arabidopsis thaliana* regulated by the *BOR1* gene. Soil Sci. Plant Nutr. **47:** 345–357.

Tanaka, M., and Fujiwara, T. (2008). Physiological roles and transport mechanisms of boron: Perspectives from plants. Pflugers Arch. **456:** 671–677.

Tyerman, S.D., Niemietz, C.M., and Bramley, H. (2002). Plant aquaporins: Multifunctional water and solute channels with expanding roles. Plant Cell Environ. **25:** 173–194.

Vincill, E.D., Szczyglowski, K., and Roberts, D.M. (2005). GmN70 and LjN70: Anion transporters of the symbiosome membrane of nodules with a transport preference for nitrate. Plant Physiol. **137:** 1435–1444.

Wallace, I.S., Choi, W.G., and Roberts, D.M. (2006). The structure, function and regulation of the nodulin 26-like intrinsic protein family of plant aquaglyceroporins. Biochim. Biophys. Acta **1758:** 1165–1175.

Wallace, I.S., and Roberts, D.M. (2004). Homology modeling of representative subfamilies of Arabidopsis major intrinsic proteins: classification based on the aromatic/arginine selectivity filter. Plant Physiol. **135:** 1059–1068.

Wallace, I.S., and Roberts, D.M. (2005). Distinct transport selectivity of two structural subclasses of the nodulin-like intrinsic protein family of plant aquaglyceroporin channels. Biochemistry **44:** 16826–16834.

Warington, K. (1923). The effect of boric acid and borax on the broad bean and certain other plants. Ann. Bot. (Lond.) **27:** 629–672.

Weaver, C.D., Crombie, B., Stacey, G., and Roberts, D.M. (1991). Calcium-dependent phosphorylation of symbiosome membrane proteins from nitrogen-fixing soybean nodules. Evidence for phosphorylation of nodulin 26. Plant Physiol. **95:** 222–227.

Woods, W.G. (1996). Review of possible boron speciation relating to its essentiality. J. Trace Elem. Exp. Med. **9:** 153–163.

Zardoya, R. (2005). Phylogeny and evolution of the major intrinsic protein family. Biol. Cell **97:** 397–414.

Zimmermann, P., Hirsch-Hoffmann, M., Hennig, L., and Gruissem, W. (2004). GENEVESTIGATOR. *Arabidopsis* microarray database and analysis toolbox. Plant Physiol. **136:** 2621–2632.